

**A label-free immunosensor for detection of nuclear matrix  
protein-22 based on Chrysanthemum-like Co-MOFs/CuAu NWs  
nanocomposite**

**Siyuan Li <sup>1</sup>, Song Yue <sup>1</sup>, Chao Yu, Yiyu Chen, Dong Yuan, Qiubo Yu \***

*Institute of Life Science, Chongqing Medical University, Chongqing 400016, P.R.  
China*

\*Corresponding author: Dr. Qiubo Yu

E-mail: yqb76712@gmail.com

Phone: (86) 23-68815186

Fax: (86) 23-68865186

<sup>1</sup> Siyuan Li and Song Yue contributed equally to this work.

Full address: 1 Yi Xue Yuan Road, Yuzhong District Chongqing, Chong Qing Medical  
University, 400016, P.R. China

## Results and discussion section

### Choice of materials

In Fig. S1, we added the three materials with the same concentration on the surface of the electrodes and then incubated them with the same concentration of antibodies. The experimental results showed that after the antibodies got attached to the materials, the Co-MOFs had no catalytic activity, and thus the current for them did not change. On the other hand, the current of the CuAu nanowires decreased and the current of the Co-MOFs/CuAu NWs was reduced more. Owing to the presence of the Co-MOFs, the Co-MOFs/CuAu NWs were able to bind more antibodies than the CuAu nanowires alone.

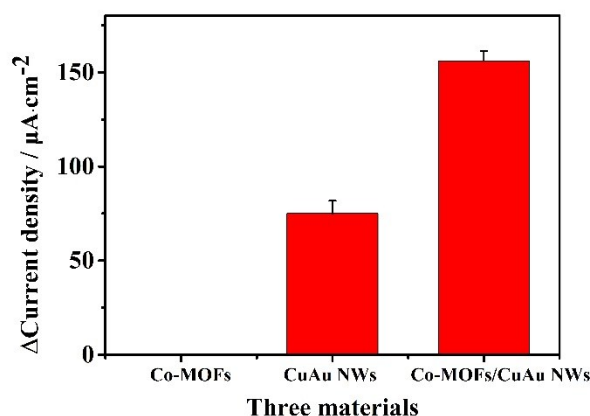


**Fig. S1.** Magnitude of the changes in the current signal after the antibodies were connected to the three materials analyzed (Co-MOFs, CuAu NWs, Co-MOFs/CuAu NWs)

### Morphological and structural characterization of the nanocomposite

To further confirm the successful synthesis of Co-MOFs/CuAu NWs nanocomposite, XPS was employed to detect the Co-MOFs/CuAu NWs nanocomposite and the results were showed in Fig. S2. In Fig. S2A, the nanocomposite showed the spectrum of C1s, O1s, Au4f, Cu2p and Co2p. The spectrum of Au4f, Co2p and Cu2p are displayed in Fig. 2B, C, and D, verifying the successful synthesis of Co-

MOFs/CuAu NWs. The results manifest that the CuAu NWs effectively anchored the Co-MOFs.

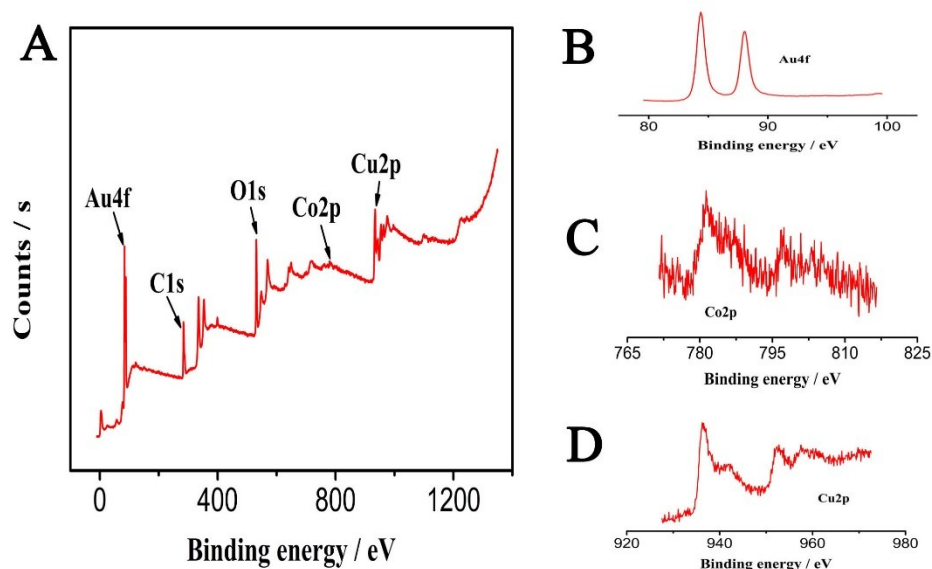


**Fig. S2.** The XPS spectrum of Co-MOFs/CuAu NWs (A), The spectra of Au4f in Co-MOFs/CuAu NWs (B), Co2p in Co-MOFs/CuAu NWs (C), and Cu2p in Co-MOFs/CuAu NWs (D).

### Optimization of experimental conditions

In practical applications, the current response of the proposed immunosensor may be influenced by many critical factors, such as the concentrations of Co-MOFs/CuAu NWs and  $\text{H}_2\text{O}_2$ , the incubation time of the antibodies, and the reaction time between the antibody and the antigen. Therefore, we optimized for the four vital requirements that would affect the results of our experiments. Figure. S3A shows the amperometric responses for different concentrations of Co-MOFs/CuAu NWs toward the reduction of  $\text{H}_2\text{O}_2$  in phosphate buffered solution (pH 7.4). For concentrations of Co-MOFs/CuAu NWs ranging from  $1.0$  to  $1.5 \text{ mol}\cdot\text{mL}^{-1}$ , the current signal gradually increased, and as the concentration was increased further, the current began to decrease. Hence,  $1.5 \text{ mol}\cdot\text{mL}^{-1}$  was selected as the optimal concentration of Co-MOFs/CuAu NWs for electrode modification in this work.

Then, the effect of the concentration of  $\text{H}_2\text{O}_2$  on electrocatalytic activity was explored, which was a significant factor that mainly affected the amperometric response. As shown in Fig. S3B, as the concentration of  $\text{H}_2\text{O}_2$  increased, the current signal gradually increased. After adding  $1.6 \text{ mol}\cdot\text{L}^{-1}$  of  $\text{H}_2\text{O}_2$ , the current changes reached a peak and then declined as the concentration was further increased. Thus,  $1.6 \text{ mol}\cdot\text{L}^{-1}$  of  $\text{H}_2\text{O}_2$  was determined to be the optimal concentration.

The time at which the antibody was immobilized on the electrode was also a very important parameter affecting the performance of the biosensor. As shown in Fig. S3C, the current signal decreased quickly upon increasing the immobilization time of anti-NMP-22 to 45min at  $37^\circ\text{C}$ , but no further decrease was observed in spite of increasing the immobilization time further, indicating that the immobilization of anti-NMP-22 had reached saturation. Therefore, 45min was determined to be the optimal immobilization time at  $37^\circ\text{C}$ .

In order to maximize the recognition of the target antigen, reaction time also plays a crucial role affecting the performance of the proposed electrochemical immunosensor. As shown in Fig. S3D, with an increase of the reaction time, the electrochemical current decreased rapidly in 1 h to 2 h and finally remained steady at approximately 2 h. Therefore, the optimal reaction time was 2 h, which was adopted in subsequent experiments.

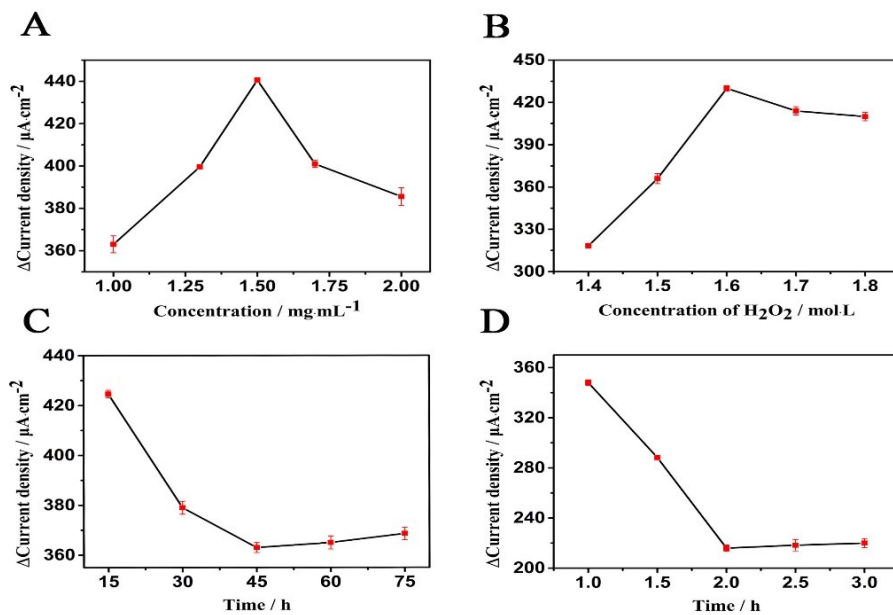


**Fig. S3.** Effects of (A) Concentration of Co-MOFs/CuAu NWs, (B) Concentration of H<sub>2</sub>O<sub>2</sub>, (C) Capture time, (D) Incubation time

### **Analytical performance of the NMP-22 sensor**

To prove that the immunosensor we designed is more advantageous than currently existing method, we tested the NMP-22 kit and plotted its standard curve. The results are shown in Fig. S4, the linear range was 5 – 80 ng·mL<sup>-1</sup> and the detection limit was 1.7 ng·mL<sup>-1</sup>. Compared with the sensors that we designed, the ELISA method had a narrower linear range, higher detection limits, and lower sensitivity. Therefore, the NMP-22 immunosensor had better performance and was very advantageous for detecting low concentrations of NMP-22.

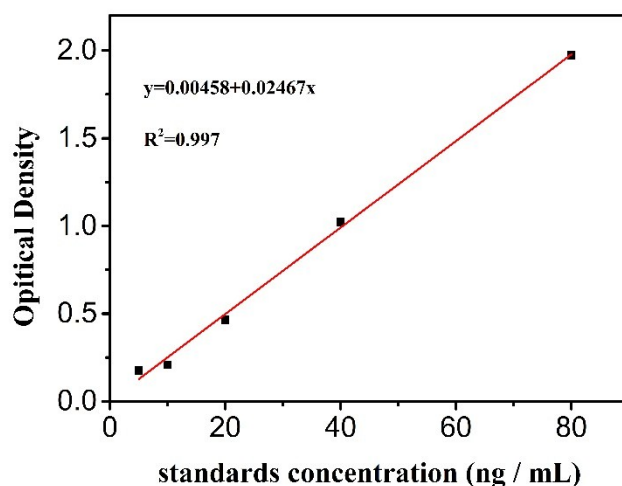


**Fig. S4.** The calibration curves of the NMP-22 kit

### **Analysis of the NMP-22 spiked human urine samples**

In order to further studies the reliability and potential application of the constructed immunosensor in actual sample, the recovery of different concentrations of NMP-22 in human urine samples was determined by standard addition method. We obtained the current of different concentrations NMP-22 by the amperometric i-t curve and the

curves of the recovery different concentrations NMP-22 were shown in Fig. S5.

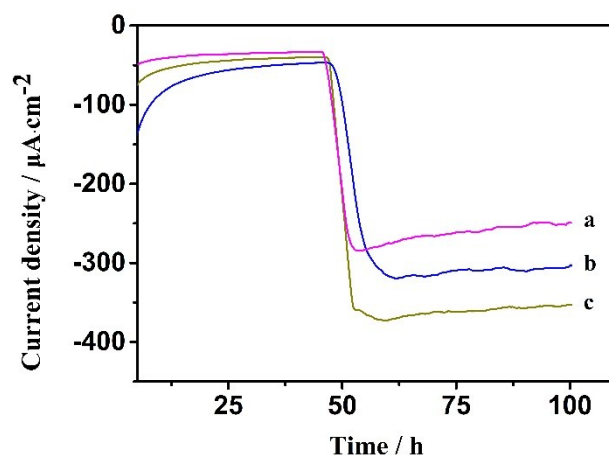


**Fig. S5.** Amperometric i-t curves of the recovery obtained with different concentrations of NMP-22: (a)  $1 \text{ ng}\cdot\text{mL}^{-1}$ ; (b)  $10 \text{ pg}\cdot\text{mL}^{-1}$ ; (c)  $100 \text{ fg}\cdot\text{mL}^{-1}$

**Table S1.** The data of EDS (Co-MOFs/CuAu NWs)

Element	Line Type	Apparent Concentration	k Ratio	Wt %	Wt % Sigma
C	K series	1.51	0.01511	8.34	0.64
O	K series	3.10	0.01042	5.77	0.35
Co	K series	0.64	0.00638	0.71	0.17
Cu	K series	13.69	0.13693	15.07	0.4
Au	M series	53.40	0.53402	70.11	0.69
Total:				100	

**Table S2.** Comparison of analytical detection results for the linear range and LOD of NMP-22

Detection technology	Linear range	Limit of detection	Refs
Electrochemical immune-biosensor	1.2–200 ng/mL	0.5 ng/mL	1
Electrochemical sensing	128–588 ng/mL	-	2
Label-free electrochemiluminescence immunosensor	0.05–2.0 ng/mL	10.0 pg/mL	3
Label-free electrochemical method	0.0001–1.0 ng/mL	33.3 fg/mL	This work

## References

1. Y. H. Chang, C. H. Wu, Y. L. Lee, P. H. Huang, Y. L. Kao and M. Y. Shiau, *Urology*, 2004, **64**, 687-692.
2. M. H. Lee, J. L. Thomas, Y. C. Chang, Y. S. Tsai, B. D. Liu and H. Y. Lin, *Biosensors & bioelectronics*, 2016, **79**, 789-795.

3. X. L. Tongqian Han, Yueyun Li, Wei Cao, Dan Wu, Bin Du, Qin Wei, *Sensors and Actuators B: Chemical*, 2014, **205**, 176-183.